

Phase-Space analysis of Teleparallel Dark Energy

Chen Xu,^{1,*} Emmanuel N. Saridakis,^{2,3,†} and Genly Leon^{4,‡}

¹*College of Mathematics and Physics,*

Chongqing University of Posts and Telecommunications, Chongqing 400065, China

²*Physics Division, National Technical University of Athens, 15780 Zografou Campus, Athens, Greece*

³*CASPER, Physics Department, Baylor University, Waco, TX 76798-7310, USA*

⁴*Department of Mathematics, Universidad Central de Las Villas, Santa Clara CP 54830, Cuba*

We perform a detailed dynamical analysis of the teleparallel dark energy scenario, which is based on the teleparallel equivalent of General Relativity, in which one adds a canonical scalar field, allowing also for a nonminimal coupling with gravity. We find that the universe can result in the quintessence-like, dark-energy-dominated solution, or to the stiff dark-energy late-time attractor, similarly to standard quintessence. However, teleparallel dark energy possesses an additional late-time solution, in which dark energy behaves like a cosmological constant, independently of the specific values of the model parameters. Finally, during the evolution the dark energy equation-of-state parameter can be either above or below -1 , offering a good description for its observed dynamical behavior and its stabilization close to the cosmological-constant value.

PACS numbers: 98.80.-k, 95.36.+x, 04.50.Kd

I. INTRODUCTION.

According to observations, the observable universe experiences an accelerating expansion at late times [1]. There are two major ways to explain such a behavior, apart from the simple consideration of a cosmological constant. The first is to modify the gravitational sector itself (see [2] for a review and references therein), obtaining a modified cosmological dynamics. The other approach is to modify the content of the universe introducing the dark energy with negative pressure, which can be based on a canonical scalar field (quintessence) [3, 4], a phantom field [5], or on the combination of both these fields in a unified scenario called quintom [6] (see the reviews [7] and [8]).

“Teleparallel” dark energy is a recently proposed scenario that tries to incorporate the dark energy sector [9, 10]. It is based on the “teleparallel” equivalent of General Relativity (TEGR), that is based on torsion instead of curvature formulation [11, 12], in which one adds a canonical scalar field, and the dark energy sector is attributed to this field. In the case where the field is minimally-coupled to gravity, the scenario is completely equivalent to standard quintessence [3], both at the background and perturbation levels. However, in the case where one switches on the nonminimal coupling between the field and the torsion scalar which is the only suitable gravitational scalar in TEGR, the resulting scenario has a richer structure, exhibiting quintessence-like or phantom-like behavior, or experiencing the phantom-divide crossing [9].

Since teleparallel dark energy exhibits interesting cos-

mological behavior, in the present work we perform a phase-space and stability analysis of such a scenario, examining in a systematic way the possible cosmological behaviors, focusing on the late-time stable solutions. Such an approach allows us to bypass the high non-linearities of the cosmological equations, which prevent any complete analytical treatment, obtaining a (qualitative) description of the global dynamics of these models, that is independent of the initial conditions and the specific evolution of the universe. Furthermore, in these asymptotic solutions we calculate various observable quantities, such as the deceleration parameter, the effective (total) equation-of-state parameter, and the various density parameters.

The plan of the work is the following: In section II we briefly review the scenario of teleparallel dark energy and in section III we perform a detailed phase-space analysis. In section IV we discuss the cosmological implications and the physical behavior of the scenario. Finally, section V is devoted to the summary of the results.

II. TELEPARALLEL DARK ENERGY

In this section we review teleparallel dark energy. Such a scenario is based on the “teleparallel” equivalent of General Relativity (TEGR)[11, 12], in which instead of using the torsionless Levi-Civita connection one uses the curvatureless Weitzenböck one. The dynamical objects are the four linearly independent, *parallel* vector fields called vierbeins, and the advantage of this framework is that the torsion tensor is formed solely from products of first derivatives of the tetrad. In particular, the vierbein field $e_A(x^\mu)$ forms an orthonormal basis for the tangent space at each point x^μ , that is $e_A \cdot e_B = \eta_{AB}$, where $\eta_{AB} = \text{diag}(1, -1, -1, -1)$, and furthermore the vector e_A can be analyzed with the use of its components e^μ_A

*Electronic address: xuc1990@126.com

†Electronic address: Emmanuel.Saridakis@baylor.edu

‡Electronic address: genly@uclv.edu.cu

in a coordinate basis, that is $\mathbf{e}_A = e_A^\mu \partial_\mu$ ¹. In such a construction, the metric tensor is obtained from the dual vierbein as

$$g_{\mu\nu}(x) = \eta_{AB} e_A^\mu(x) e_B^\nu(x). \quad (1)$$

Furthermore, the torsion tensor of the Weitzenböck connection $\overset{\mathbf{w}}{\Gamma}_{\nu\mu}^\lambda$ [14] reads

$$T_{\mu\nu}^\lambda = \overset{\mathbf{w}}{\Gamma}_{\nu\mu}^\lambda - \overset{\mathbf{w}}{\Gamma}_{\mu\nu}^\lambda = e_A^\lambda (\partial_\mu e_\nu^A - \partial_\nu e_\mu^A). \quad (2)$$

In the present formalism all the information concerning the gravitational field is included in the torsion tensor $T_{\mu\nu}^\lambda$. The corresponding “teleparallel Lagrangian” can be constructed from this torsion tensor under the assumptions of invariance under general coordinate transformations, global Lorentz transformations, and the parity operation, along with requiring the Lagrangian density to be second order in the torsion tensor [12]. In particular, it is proved to be just the torsion scalar T , namely [11, 12, 15]:

$$\mathcal{L} = T = \frac{1}{4} T^{\rho\mu\nu} T_{\rho\mu\nu} + \frac{1}{2} T^{\rho\mu\nu} T_{\nu\mu\rho} - T_{\rho\mu}^\rho T^{\nu\mu}_\nu. \quad (3)$$

Therefore, the simplest action in a universe governed by teleparallel gravity is

$$I = \int d^4x e \left[\frac{T}{2\kappa^2} + \mathcal{L}_m \right], \quad (4)$$

where $e = \det(e_\mu^A) = \sqrt{-g}$ (one could also include a cosmological constant). Variation with respect to the vierbein fields gives the equations of motion, which are exactly the same as those of General Relativity for every geometry choice, and that is why the theory is called “teleparallel equivalent to General Relativity”.

In principle one has two ways of generalizing the action (4), inspired by the corresponding procedures of standard General Relativity. The first is to replace T by an arbitrary function $f(T)$ [13, 16], similarly to $f(R)$ extensions of GR, and obtain new interesting terms in the field equations. The other, on which we focus in this work, is to add a canonical scalar field in (4), similarly to GR quintessence, allowing for a nonminimal coupling with gravity. Then the dark energy sector will be attributed to this field and therefore the corresponding scenario is called “teleparallel dark energy” [9]. In particular, the action will simply read:

$$S = \int d^4x e \left[\frac{T}{2\kappa^2} + \frac{1}{2} (\partial_\mu \phi \partial^\mu \phi + \xi T \phi^2) - V(\phi) + \mathcal{L}_m \right]. \quad (5)$$

Concerning the nonminimal coupling we emphasize that since inTEGR, that is in the torsion formulation of GR, the only scalar is the torsion one, the nonminimal coupling will be between this and the scalar field (similarly to standard nonminimal quintessence where the scalar field couples to the Ricci scalar).

Variation of action (5) with respect to the vierbein fields yields equation of motion

$$\begin{aligned} \left(\frac{2}{\kappa^2} + 2\xi\phi^2 \right) & \left[e^{-1} \partial_\mu (e e_A^\rho S_\rho^{\mu\nu}) - e_A^\lambda T^\rho_{\mu\lambda} S_\rho^{\nu\mu} - \frac{1}{4} e_A^\nu T \right] \\ & - e_A^\nu \left[\frac{1}{2} \partial_\mu \phi \partial^\mu \phi - V(\phi) \right] + e_A^\mu \partial^\nu \phi \partial_\mu \phi \\ & + 4\xi e_A^\rho S_\rho^{\mu\nu} \phi (\partial_\mu \phi) = e_A^\rho \overset{\text{em}}{T}_\rho{}^\nu. \end{aligned} \quad (6)$$

where $\overset{\text{em}}{T}_\rho{}^\nu$ stands for the usual energy-momentum tensor. Therefore, imposing a flat Friedmann-Robertson-Walker (FRW) background metric

$$ds^2 = dt^2 - a^2(t) \delta_{ij} dx^i dx^j, \quad (7)$$

where t is the cosmic time, x^i are the comoving spatial coordinates and $a(t)$ is the scale factor, that is for a vierbein choice of the form

$$e_\mu^A = \text{diag}(1, a, a, a), \quad (8)$$

we obtain the corresponding Friedmann equations:

$$H^2 = \frac{\kappa^2}{3} (\rho_\phi + \rho_m), \quad (9)$$

$$\dot{H} = -\frac{\kappa^2}{2} (\rho_\phi + p_\phi + \rho_m + p_m), \quad (10)$$

where $H = \dot{a}/a$ is the Hubble parameter, a dot denotes differentiation with respect to t . In these expressions, ρ_m and p_m are the matter energy density and pressure, respectively, following the standard evolution equation $\dot{\rho}_m + 3H(1 + w_m)\rho_m = 0$, with $w_m = p_m/\rho_m$ the matter equation-of-state parameter. Furthermore, we have introduced the effective energy density and pressure of scalar field

$$\rho_\phi = \frac{1}{2} \dot{\phi}^2 + V(\phi) - 3\xi H^2 \phi^2, \quad (11)$$

$$p_\phi = \frac{1}{2} \dot{\phi}^2 - V(\phi) + 4\xi H \phi \dot{\phi} + \xi (3H^2 + 2\dot{H}) \phi^2. \quad (12)$$

Moreover, variation of the action with respect to the scalar field provides its evolution equation, namely:

$$\ddot{\phi} + 3H\dot{\phi} + 6\xi H^2 \phi + V'(\phi) = 0. \quad (13)$$

Note that in the above expressions we have used the useful relation

$$T = -6H^2, \quad (14)$$

which straightforwardly arises from the calculation of (3) for the flat FRW geometry.

¹ We follow the notation of [13], that is Greek indices μ, ν, \dots and capital Latin indices A, B, \dots run over all coordinate and tangent space-time $0, 1, 2, 3$, while lower case Latin indices (from the middle of the alphabet) i, j, \dots and lower case Latin indices (from the beginning of the alphabet) a, b, \dots run over spatial and tangent space coordinates $1, 2, 3$, respectively. Finally, we use the metric signature $(+, -, -, -)$.

In this scenario, similarly to the standard quintessence, dark energy is attributed to the scalar field, and thus its equation-of-state parameter (w_{DE}) reads:

$$w_{DE} \equiv w_\phi = \frac{p_\phi}{\rho_\phi}. \quad (15)$$

Finally, one can see that the scalar field evolution (13) leads to the standard relation

$$\dot{\rho}_\phi + 3H(1 + w_\phi)\rho_\phi = 0. \quad (16)$$

Teleparallel dark energy exhibits very interesting cosmological behavior. In the minimally-coupled case the cosmological equations coincide with those of the standard quintessence, both at the background and perturbation levels. However, in the nonminimal case one can obtain a dark energy sector being quintessence-like, phantom-like, or experiencing the phantom-divide crossing during evolution, a behavior that is much richer comparing to General Relativity (GR) with a scalar field [9, 10]. Therefore, it is both interesting and necessary to perform a phase-space analysis, that is to investigate late-time solutions that are independent from the initial conditions and the specific universe evolution. This is performed in the next section.

III. PHASE-SPACE ANALYSIS

In order to perform the phase-space and stability analysis of the scenario at hand, we have to transform the aforementioned dynamical system into its autonomous form $\mathbf{X}' = \mathbf{f}(\mathbf{X})$ [17, 18], where \mathbf{X} is the column vector constituted by suitable auxiliary variables, $\mathbf{f}(\mathbf{X})$ the corresponding column vector of the autonomous equations, and prime denotes derivative with respect to $M =$

$\ln a$. Then we extract its critical points \mathbf{X}_c satisfying $\mathbf{X}' = \mathbf{0}$, and in order to determine the stability properties of these critical points, we expand around \mathbf{X}_c , setting $\mathbf{X} = \mathbf{X}_c + \mathbf{U}$, with \mathbf{U} the perturbations of the variables considered as a column vector. Thus, for each critical point we expand the equations for the perturbations up to the first order as: $\mathbf{U}' = \mathbf{Q} \cdot \mathbf{U}$, where the matrix \mathbf{Q} contains the coefficients of the perturbation equations. Finally, for each critical point, the eigenvalues of \mathbf{Q} determine its type and stability.

In the scenario at hand, we introduce the auxiliary variables:

$$\begin{aligned} x &= \frac{\kappa \dot{\phi}}{\sqrt{6}H} \\ y &= \frac{\kappa \sqrt{V(\phi)}}{\sqrt{3}H} \\ z &= \sqrt{|\xi|} \kappa \phi. \end{aligned} \quad (17)$$

Using these variables the Friedmann equation (9) becomes

$$x^2 + y^2 - z^2 \text{sgn}(\xi) + \frac{\kappa^2 \rho_m}{3H^2} = 1. \quad (18)$$

This constraint allows for expressing ρ_m as a function of the auxiliary variables (17). Therefore, using (18) and (11) we can write the density parameters as:

$$\begin{aligned} \Omega_m &\equiv \frac{\kappa^2 \rho_m}{3H^2} = 1 - x^2 - y^2 + z^2 \text{sgn}(\xi) \\ \Omega_{DE} &\equiv \frac{\kappa^2 \rho_\phi}{3H^2} = x^2 + y^2 - z^2 \text{sgn}(\xi), \end{aligned} \quad (19)$$

while for the dark-energy equation-of-state parameter (15) we obtain:

$$w_{DE} = \frac{x^2 - y^2 + 4\sqrt{\frac{2}{3}}zx\sqrt{|\xi|}\text{sgn}(\xi) - z^2w_m\text{sgn}(\xi) [1 - x^2 - y^2 + z^2\text{sgn}(\xi)]}{[1 + z^2 \text{sgn}(\xi)] [x^2 + y^2 - z^2\text{sgn}(\xi)]}. \quad (20)$$

In this scenario w_{DE} can be quintessence-like, phantom-like, or experience the phantom divide crossing during the evolution. Without loss of generality, in the following we restrict the analysis in the dust matter case, that is we assume that $w_m = 0$.

It is convenient to introduce two additional quantities with great physical significance, namely the “total” equation-of-state parameter:

$$w_{tot} \equiv \frac{p_\phi}{\rho_\phi + \rho_m} = w_{DE} \Omega_{DE} = \frac{x^2 - y^2 + 4\sqrt{\frac{2}{3}}zx\sqrt{|\xi|}\text{sgn}(\xi)}{1 + z^2 \text{sgn}(\xi)}, \quad (21)$$

and the deceleration parameter q :

$$\begin{aligned} q &\equiv -1 - \frac{\dot{H}}{H^2} = \frac{1}{2} + \frac{3}{2}w_{tot} \\ &= \frac{1 + 3(x^2 - y^2) + [z + 4\sqrt{6}x\sqrt{|\xi|}] z \text{sgn}(\xi)}{2 [1 + z^2 \text{sgn}(\xi)]}. \end{aligned} \quad (22)$$

Finally, concerning the scalar potential $V(\phi)$ the usual assumption in the literature is to assume an exponential potential of the form

$$V = V_0 \exp(-\kappa \lambda \phi), \quad (23)$$

since exponential potentials are known to be significant in various cosmological models [17, 18] (equivalently, but more generally, we could consider potentials satisfying $\lambda = -\frac{1}{\kappa V(\phi)} \frac{\partial V(\phi)}{\partial \phi} \approx \text{const}$, which is valid for arbitrary but nearly flat potentials [19]). Moreover, note that the exponential potential was used as an example in the initial work on teleparallel dark energy [9].

In summary, using the auxiliary variables (17) and considering the exponential potential (23), the equations of motion (9), (10) and (13) in the case of dust matter, can be transformed into the following autonomous system:

$$\begin{aligned} x' &= \frac{3x^3}{2z^2 \text{sgn}(\xi) + 2} + \frac{2\sqrt{6}z\sqrt{|\xi|}x^2 \text{sgn}(\xi)}{z^2 \text{sgn}(\xi) + 2} - \frac{3x}{2} \\ &\quad + \frac{1}{2}y^2 \left[\sqrt{6}\lambda - \frac{3x}{\text{sgn}(\xi)z^2 + 1} \right] - \sqrt{6}z\sqrt{|\xi|} \text{sgn}(\xi) \\ y' &= \frac{3yx^2}{2 \text{sgn}(\xi)z^2 + 2} + \frac{3}{2}y \left[1 - \frac{y^2}{z^2 \text{sgn}(\xi) + 1} \right] \\ &\quad - \frac{\sqrt{\frac{3}{2}}yx \left\{ \left[\lambda z - 4\sqrt{|\xi|} \right] z \text{sgn}(\xi) + \lambda \right\}}{1 + z^2 \text{sgn}(\xi)} \\ z' &= \sqrt{6}\sqrt{|\xi|x}, \end{aligned} \quad (24)$$

where we have used that for every quantity F we acquire $\dot{F} = HF'$. Since ρ_m is nonnegative, from (18) we obtain that $x^2 + y^2 - z^2 \text{sgn}(\xi) \leq 1$. Thus, we deduce that for $\xi < 0$ the system (24) defines a flow on the compact phase space $\Psi = \{x^2 + y^2 - z^2 \text{sgn}(\xi) \leq 1, y \geq 0\}$, for $\xi = 0$ the phase space is compact and it is reduced to the circle $\Psi = \{x^2 + y^2 \leq 1, y \geq 0\}$, while for $\xi > 0$ the phase space Ψ is unbounded.

Before proceeding we make two comments on the degrees of freedom and the choice of auxiliary variables. Firstly, as we have already mentioned, in the minimal coupling case, that is when $\xi = 0$, the model at hand coincides with standard quintessence, which phase space analysis is well known using two degrees of freedom, namely the variables x and y defined above [17]. On the other hand, when $\xi \neq 0$ we have three degrees of freedom and all x, y, z are necessary. Therefore, in order to perform the analysis in a unified way, we use the three variables defined above, having in mind that for $\xi = 0$ the variable z becomes zero and thus irrelevant. Secondly, apart from the standard choices of the variables x and y , one must be careful in suitably choosing the variable z in order not to lose dynamical information. For example, although the choice for the variable $z = \frac{\kappa \rho_m}{\sqrt{3}H}$ is another reasonable choice, however it still loses the critical points that lie at “infinity”. Therefore, in order to completely cover the phase-space behavior in the following we will additionally use the Poincaré central projection method to investigate the dynamics at “infinity”. The negligence of this point was the reason of the incomplete phase space analysis of teleparallel dark energy performed in [20].

A. Finite Phase-space analysis

Let us now proceed to the phase-space analysis. The real and physically meaningful (that is corresponding to an expanding universe, i.e. possessing $H > 0$) critical points (x_c, y_c, z_c) of the autonomous system (24), obtained by setting the left hand sides of the equations to zero, are presented in Table I. In the same table we provide the conditions for their existence. The 3×3 matrix \mathbf{Q} of the linearized perturbation equations of the system (24) is shown in Appendix A. For each critical point of Table I we examine the sign of the real part of the eigenvalues of \mathbf{Q} in order to determine the type and stability of the point. The details of the analysis and the various eigenvalues are presented in Appendix A, and in Table I we summarize the results.² In addition, for each critical point we calculate the values of Ω_{DE} , w_{DE} , w_{tot} and q given by (19), (20), (21) and (22) respectively.

B. Phase-space analysis at infinity

Due to the fact that the dynamical system (24) is non-compact for the choice $\xi > 0$, there could be features in the asymptotic regime which are non-trivial for the global dynamics. Thus, in order to complete the analysis of the phase space we must extend our study using the Poincaré central projection method [21].

Let us consider the Poincaré variables

$$x_r = \rho \cos \theta \sin \psi, \quad z_r = \rho \sin \theta \sin \psi, \quad y_r = \rho \cos \psi, \quad (25)$$

where $\rho = \frac{r}{\sqrt{1+r^2}}$, $r = \sqrt{x^2 + y^2 + z^2}$, $\theta \in [0, 2\pi]$, and $-\frac{\pi}{2} \leq \psi \leq \frac{\pi}{2}$ (we restrict the angle ψ to this interval since the physical region is given by $y > 0$). Thus, the points at “infinity” ($r \rightarrow +\infty$) are those having $\rho \rightarrow 1$. Furthermore, the physical phase space is given by

$$\left\{ (x_r, y_r, z_r) \in [-1, 1] \times [0, 1] \times [-1, 1] \mid z_r^2 \leq x_r^2 + y_r^2 \leq \frac{1}{2} \right\}.$$

Inverting relations (25) and substituting into (19), (20), we obtain the dark energy density and equation-of-state parameters as a function of the Poincaré variables, namely:

$$\Omega_{DE} = \frac{x_r^2 + y_r^2 - z_r^2}{1 - x_r^2 - y_r^2 - z_r^2} \quad (26)$$

$$w_{DE} = \frac{(3x_r^2 + 4\sqrt{6}\sqrt{|\xi|}z_r x_r - 3y_r^2)(1 - x_r^2 - y_r^2 - z_r^2)}{3(1 - x_r^2 - y_r^2)(x_r^2 + y_r^2 - z_r^2)}, \quad (27)$$

² The critical point D that exists only for $\xi = 0$, is very close to be a stationary point in the general case ($\xi \neq 0$) too, but with an arbitrarily small value of the slope of the potential λ . It becomes an exact critical point only for $\lambda = 0$, namely the point J . Furthermore, for arbitrary large values of λ the singular point E (that exists for $\xi = 0$) mimics the behavior of the point A (that exists for $\xi \neq 0$).

Cr. P.	x_c	y_c	z_c	Exists for	Stability	Ω_{DE}	w_{DE}	w_{tot}	q
A	0	0	0	all ξ, λ	saddle point	0	arbitrary	0	$\frac{1}{2}$
B	1	0	0	$\xi = 0$, all λ	unstable for $\lambda < \sqrt{6}$ saddle point otherwise	1	1	1	2
C	-1	0	0	$\xi = 0$, all λ	unstable for $\lambda > -\sqrt{6}$ saddle point otherwise	1	1	1	2
D	$\frac{\lambda}{\sqrt{6}}$	$\sqrt{1 - \frac{\lambda^2}{6}}$	0	$\xi = 0$, $\lambda^2 \leq 6$	stable node for $\lambda^2 < 3$ saddle point for $3 < \lambda^2 < 6$	1	$-1 + \frac{\lambda^2}{3}$	$-1 + \frac{\lambda^2}{3}$	$-1 + \frac{\lambda^2}{2}$
E	$\sqrt{\frac{3}{2}\lambda}$	$\sqrt{\frac{3}{2}\lambda}$	0	$\xi = 0$, $\lambda^2 \geq 3$	stable node for $3 < \lambda^2 < \frac{24}{7}$ stable spiral for $\lambda^2 > \frac{24}{7}$	$\frac{3}{\lambda^2}$	0	0	$\frac{1}{2}$
F	0	$\sqrt{\frac{2\xi - 2\sqrt{\xi(\xi - \lambda^2)}}{\lambda^2}}$	$\frac{\xi - \sqrt{\xi(\xi - \lambda^2)}}{\lambda\xi} \sqrt{ \xi }$	$0 < \lambda^2 \leq \xi$	stable node for $\lambda^2 < \xi$	1	-1	-1	-1
G	0	$\sqrt{\frac{2\xi + 2\sqrt{\xi(\xi - \lambda^2)}}{\lambda^2}}$	$\frac{\xi + \sqrt{\xi(\xi - \lambda^2)}}{\lambda\xi} \sqrt{ \xi }$	$0 < \lambda^2 \leq \xi$ or $\xi < 0$	saddle point	1	-1	-1	-1
J	0	1	0	$\xi \neq 0$ and $\lambda = 0$	stable spiral for $\frac{3}{8} < \xi$ stable node for $0 < \xi < \frac{3}{8}$ saddle point for $\xi < 0$	1	-1	-1	-1

TABLE I: The real and physically meaningful critical points of the autonomous system (24), and the corresponding values of the dark-energy density parameter Ω_{DE} , of the dark-energy equation-of-state parameter w_{DE} , of the total equation-of-state parameter w_{tot} and of the deceleration parameter q .

Cr. P.	x_{rc}	y_{rc}	z_{rc}	Stability	Ω_{DE}	w_{DE}	w_{tot}	q
K_{\pm}	$\mp \frac{\sqrt{2}}{2}$	0	$\pm \frac{\sqrt{2}}{2}$	unstable for $0 < \xi < \frac{3}{8}$ saddle point for $\frac{3}{8} < \xi$	arbitrary	arbitrary	$1 - 4\sqrt{\frac{2\xi}{3}}$	$2 - 2\sqrt{6\xi}$
L_{\pm}	$\pm \frac{\sqrt{2}}{2}$	0	$\pm \frac{\sqrt{2}}{2}$	saddle point for all $\xi > 0$	arbitrary	arbitrary	$1 + 4\sqrt{\frac{2\xi}{3}}$	$2 + 2\sqrt{6\xi}$

TABLE II: The real and physical critical points of the autonomous system (24) at infinity, which exists for $\xi > 0$, all λ , and the corresponding values of the dark-energy density parameter Ω_{DE} , of the dark-energy equation-of-state parameter w_{DE} , of the total equation-of-state parameter w_{tot} and of the deceleration parameter q .

and similarly substituting into (21), (22) we obtain the corresponding expressions for the total equation-of-state and deceleration parameters:

$$w_{tot} = \frac{3x_r^2 + 4\sqrt{6}\sqrt{\xi}z_r x_r - 3y_r^2}{3(1 - x_r^2 - y_r^2)}, \quad (28)$$

$$q = \frac{1}{2} + \frac{3}{2} \left\{ \frac{3x_r^2 + 4\sqrt{6}\sqrt{\xi}z_r x_r - 3y_r^2}{3(1 - x_r^2 - y_r^2)} \right\}. \quad (29)$$

Applying the procedure prescribed in Appendix B we conclude that there are four physical critical points at infinity, namely the points K_{\pm} , satisfying $\cot \theta = -1$, and the points L_{\pm} satisfying $\cot \theta = 1$. These critical points, along with their stability conditions are presented in Table II. In the same Table we include the corresponding values of the observables Ω_{DE} , w_{DE} , w_{tot} and q , calculated using (26),(27),(28),(29).

As we show in Appendix B, the above critical points

correspond to the limit

$$|\phi| \rightarrow \infty, \quad \left| \frac{\dot{\phi}}{H} \right| \rightarrow \infty, \quad (30)$$

satisfying the rate $(\ln \phi)' \equiv \sqrt{6} \frac{z}{z} = \sqrt{6} \cot \theta$.

IV. COSMOLOGICAL IMPLICATIONS

Having performed the complete phase-space analysis of teleparallel dark energy, we can now discuss the corresponding cosmological behavior. A first remark is that in the minimal case (that is $\xi = 0$) we do verify that the scenario at hand coincides completely with standard quintessence. Therefore, we will make a brief review on the subject and then focus on the nonminimal case.

The points B to E exists only for the minimal case, that is only for $\xi = 0$. Points B and C are not stable, corresponding to a non-accelerating, dark-energy dominated universe, with a stiff dark-energy equation-of-state

parameter equal to 1. Both of them exist in standard quintessence [17].

Point D is a saddle one for $3 < \lambda^2 < 6$, however for $0 < \lambda^2 < 3$ it is a stable node, and thus it can attract the universe at late times. It corresponds to a dark-energy dominated universe, with a dark-energy equation-of-state parameter lying in the quintessence regime, which can be accelerating or not according to the λ -value. This point exists in standard quintessence [17]. It is the most important one in that scenario, since it is both stable and possesses a w_{DE} compatible with observations.

Point E is a stable one for $3 < \lambda^2$. It has the advantage that the dark-energy density parameter lies in the interval $0 < \Omega_{DE} < 1$, that is it can alleviate the coincidence problem, since dark matter and dark energy density parameters can be of the same order (in order to treat the coincidence problem one must explain why the present dark energy and matter density parameters are of the same order of magnitude although they follow different evolution behaviors). However, it has the disadvantage that w_{DE} is 0 and the expansion is not accelerating, which are not favored by observations. This point exists in standard quintessence [17].

Let us now analyze the case $\xi \neq 0$. In this case we obtain the critical points A , F , G and J . The point A is saddle point, and thus it cannot be late-time solution of the universe. It corresponds to a non-accelerating, dark-matter dominated universe, with arbitrary dark-energy equation-of-state parameter. Note that this trivial point exists in the standard quintessence model too [17], since it is independent of ξ .

The present scenario of teleparallel dark energy, possesses two additional, non-trivial critical points that do not exist in standard quintessence. Thus, they account for the new information of this richer scenario, and as expected they depend on the nonminimal coupling ξ . In particular, point F is stable if $\lambda^2 < \xi$, and thus it can attract the universe at late times. It corresponds to an accelerating universe with complete dark energy domination, with $w_{DE} = -1$, that is dark energy behaves like a cosmological constant. We stress that this w_{DE} value is independent of λ and ξ , which is an important and novel result. Thus, while point D (the important point of standard quintessence) needs to have a very flat, that is quite tuned, potential in order to possess a w_{DE} near the observed value -1 , point F exhibits this behavior for every λ -value, provided that $\lambda^2 < \xi$. This feature is a significant advantage of the scenario at hand, amplifying its generality, and offers a mechanism for the stabilization of w_{DE} close to the cosmological-constant value. Similarly, we have the point G , which has the same cosmological properties with F , however it is a saddle point and thus it cannot be a late-time solution of the universe, but the universe can spend a large period of time near this solution.

Finally, when $\xi \neq 0$ and for the limiting case $\lambda = 0$, that is for a constant potential, the present scenario exhibits the critical point J , which is stable for $\xi > 0$. It

corresponds to a dark-energy dominated, de Sitter universe, in which dark energy behaves like a cosmological constant.

Let us now analyze the critical points at infinity. The points K_{\pm} are saddle for $\xi > \frac{3}{8}$. The fact that they possess arbitrary Ω_{DE} and w_{DE} is a significant advantage, since such solutions can alleviate the coincidence problem. Note however that the corresponding w_{tot} and deceleration parameter are not arbitrary, offering a good quantitative description of the cosmological behavior (actually this is the reason we introduced these observables). In particular, we conclude that for $\xi > \frac{1}{6}$ we obtain an accelerated expansion, while for $\xi > \frac{3}{8}$ the expansion is super-accelerating ($q < -1$ that is $\dot{H} > 0$ and $w_{tot} < -1$) that is the universe presents a phantom behavior. We mention that since these points are saddle they cannot attract the universe at late times, however the universe can spend a large period of time near these solutions, before approaching the saddle point A or the global attractor F (for potentials with slope $\lambda^2 \leq \xi$). In that case the above physical features present a transient character, which is quite significant from the observational point of view.

Points L_{\pm} are saddle for all $\xi > 0$. They have arbitrary Ω_{DE} and w_{DE} however they correspond to a non-accelerating expansion, and thus they could be important only as transient states of the universe.

In order to present the aforementioned behavior more transparently, we first evolve the autonomous system (24) numerically for the choice $\lambda = 1$, and $\xi = 0$, that is in the minimal scenario, and in Fig. 1 we depict the corresponding phase-space behavior, projected in the $x-y$ plane. As we can see, in this case the quintessence-like critical point D is the late-time solution of the universe. Note that this point exists only for the minimal case ($\xi = 0$), where our model coincides with standard quintessence (see Fig. 2 of [17]).

As we mentioned above, the late-time attractors D and E exists only for the case $\xi = 0$. To illustrate how sensible is the scenario at hand in slight changes of ξ , in Fig. 2 we depict the projection of the phase-space evolution on the $x-y$ plane, for $\lambda = 2$ and $\xi = -10^{-3}$. In this case the point E becomes “quasi-stationary”, since typical trajectories remain very close to it for a large but finite time interval, while D becomes also quasi-stationary, but it is unstable to perturbations in the z -axis.³

Finally, to illustrate the dynamics for positive ξ , which is expressed through points at “infinity”, in Fig. 3 we present the three-dimensional Poincaré (global) phase space for $\lambda = 0.5$ and $\xi = 1$. According to Table II the critical points K_{\pm} are saddle ones and exhibit phantom behavior, while L_{\pm} are saddle with a stiff dark energy sec-

³ Although the singular points B, C, D and E do not exist as critical points for the choices $\xi \neq 0$, in Fig. 2 we mark their locations explicitly, for comparison with the case $\xi = 0$ of Fig. 1.

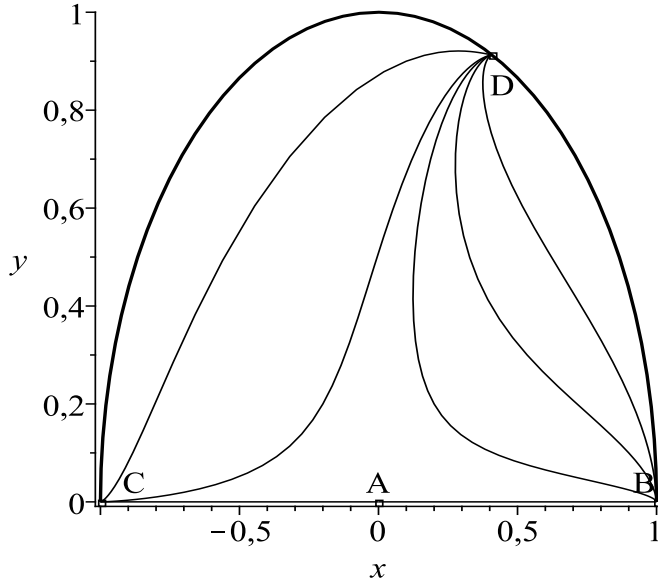


FIG. 1: The projection of the phase-space evolution on the x - y plane, for the teleparallel dark energy scenario with $\lambda = 1$ and $\xi = 0$. The trajectories are attracted by the quintessence-like stable point D , which exists only in the minimal case ($\xi = 0$).

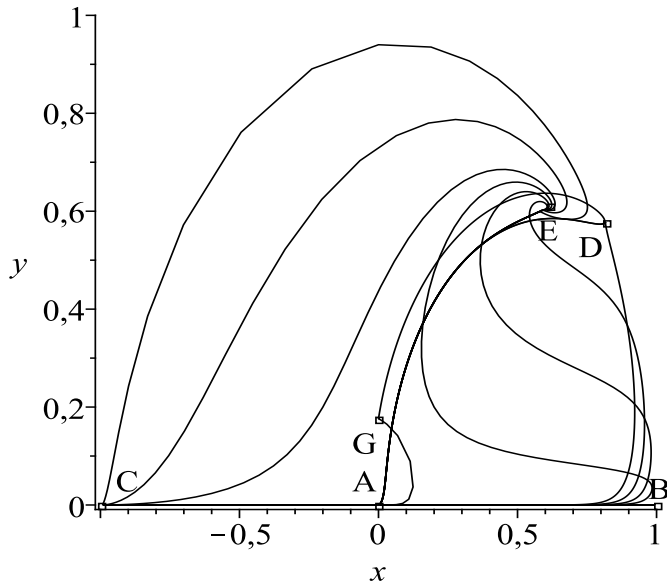


FIG. 2: The projection of the phase-space evolution on the x - y plane, for the teleparallel dark energy scenario with $\lambda = 2$ and $\xi = -10^{-3}$. Observe that an open set of trajectories remains very close to the quasi-stationary solution E , before approaching an invariant arc above the saddle point A . The critical point G is a saddle one.

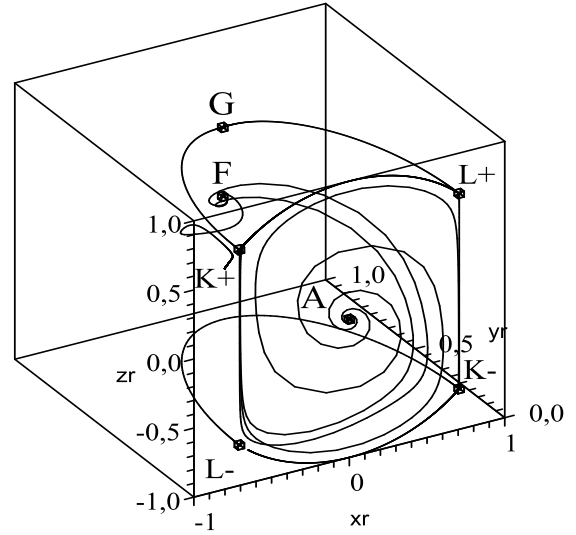


FIG. 3: Poncaré (global) phase space for the teleparallel dark energy scenario with $\lambda = 0.5$ and $\xi = 1$. The points at infinity K_{\pm}, L_{\pm} are saddles. The trajectories on both finite and infinite regions are finally attracted by the cosmological-constant-like stable point F (global attractor), having passed through matter-dominated solutions or solutions with comparable dark matter and dark energy sectors.

tor. Thus, far from their basin of attraction (but inside the invariant set $y_r = 0$) the orbits depart from them to approach the matter-dominated solution A , while for $y_r > 0$ the orbits are attracted by the cosmological-constant-like solution F . Thus, the epoch sequence $K_- \rightarrow L_+ \rightarrow K_+ \rightarrow L_- \rightarrow A \rightarrow F$ represents the transition from a universe with a phantom-like dark energy, to a matter-dominated universe with non-phantom dark energy, and then to a dark-energy-dominated, cosmological-constant-like solution. This sequence has a great cosmological significance, since it can describe the epoch sequence inflation, dark-matter domination, dark-energy domination, in agreement with observations. Additionally, the epoch sequence $L_- \rightarrow K_+ \rightarrow F$ represents the transition from a universe with comparable dark matter and dark energy sectors, to a cosmological-constant-like solution.

Before closing this section, let us make a comment on another crucial difference of teleparallel dark energy, comparing with standard quintessence, that is of the $\xi \neq 0$ case comparing to the $\xi = 0$ one. In particular, when $\xi = 0$, in which teleparallel dark energy coincides with standard quintessence, w_{DE} is always larger than -1 , not only at the critical points, but also throughout the cosmological evolution as well. However, for $\xi \neq 0$, during the cosmological evolution w_{DE} can be either above or below -1 , and only at the stable critical point it becomes equal to -1 . Such a cosmological

behavior is much richer, and very interesting, both from the theoretical as well as from the observational point of view, since it can explain the dynamical behavior of w_{DE} either above or below the phantom divide, and moreover its stabilization to the cosmological-constant value.

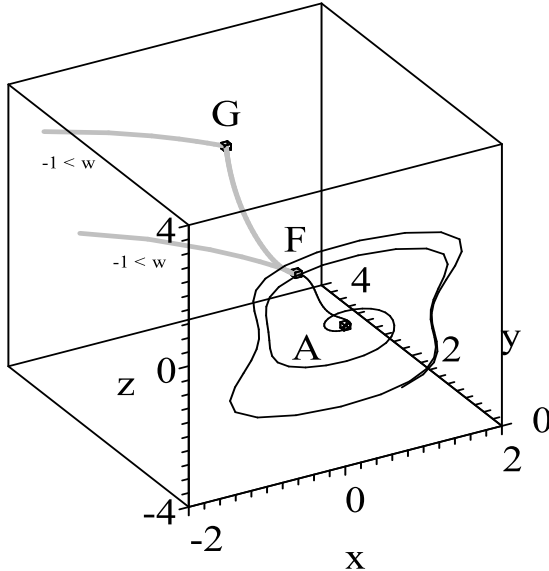


FIG. 4: The phase-space evolution for the teleparallel dark energy scenario with $\lambda = 0.7$ and $\xi = 1$. The trajectories are attracted by the cosmological-constant-like stable point F , however the evolution towards it possesses a w_{DE} being quintessence-like, phantom-like, or experiencing the phantom-divide crossing, depending on the specific initial conditions. The orbits with a thick gray curve on the top left are those with $w_{DE} > -1$ initially, while the thin black curve corresponds to $w_{DE} < -1$ initially.

In order to present the novel features of the scenario at hand, in Fig. 4 we depict the three-dimensional phase-space behavior for the choice $\lambda = 0.7$ and $\xi = 1$. In this case the universe at late times is attracted by the cosmological-constant-like stable point F . However, during the evolution towards this point the dark-energy equation-of-state parameter w_{DE} presents a very interesting behavior, and in particular, depending on the specific initial conditions, it can be quintessence-like, phantom-like, or experience the phantom-divide crossing. Such a behavior is much richer than standard quintessence, and reveals the capabilities of teleparallel dark energy scenario.

V. CONCLUSIONS

In the present work we investigated the dynamical behavior of the recently proposed scenario of teleparallel

dark energy [9, 10], which is based on the teleparallel equivalent of General Relativity (TEGR), that is on its torsion instead of curvature formulation [11, 12]. In this model one adds a canonical scalar field, in which the dark energy sector is attributed, allowing also for a nonminimal coupling between the field and the torsion scalar. Thus, although the minimal case is completely equivalent with standard quintessence, the nonminimal scenario has a richer structure, exhibiting quintessence-like or phantom-like behavior, or experiencing the phantom-divide crossing [9, 10].

Performing a detailed phase-space analysis of teleparallel dark energy, we saw that the standard quintessence-like, late-time solution [17] exists only for $\xi = 0$, and we showed that this solution becomes quasi-stationary if ξ is perturbed even slightly. The same results hold for the other standard quintessence solution, namely the stiff dark-energy late-time attractor, in which dark energy and dark matter can be of the same order, thus alleviating the coincidence problem.

Apart from the above late time solutions that exist also in the standard quintessence scenario, teleparallel dark energy has an additional and physically very interesting late-time behavior. In particular, it possesses a late-time attractor in which dark energy behaves like a cosmological constant, independently of the specific values of the model parameters (provided that the nonminimal coupling ξ is larger than the square of the potential exponent). This feature is a significant advantage of the scenario at hand, amplifying its generality, since it provides a natural way for the stabilization of the dark energy equation-of-state parameter to the cosmological constant value, without the need for parameter-tuning.

Additionally, we showed that teleparallel dark energy admits critical points at “infinity”, which are saddle for $\xi > \frac{3}{8}$, and thus although they cannot be the late-time solutions, the universe can spend a large period of time near them. Thus, one can obtain the transition from a universe with a phantom-like dark energy, to a matter-dominated universe with non-phantom dark energy, and then to a dark-energy-dominated, cosmological-constant-like solution. This sequence has a great cosmological significance, since it can describe the epoch sequence inflation, dark-matter domination, dark-energy domination, in agreement with observations.

Finally, perhaps the most interesting feature of teleparallel dark energy is that in the nonminimal case the dark energy equation-of-state parameter can be either above or below -1 , and only at the stable critical points it becomes equal to -1 . Such a cosmological behavior is much richer comparing to standard quintessence, and very interesting, both from the theoretical as well as from the observational point of view, since it can explain the dynamical behavior of w_{DE} either above or below the phantom divide, and moreover its stabilization to the cosmological-constant value. All these features make the teleparallel dark energy a good candidate for the description of dark energy.

Acknowledgments

The authors would like to thank Yungui Gong for crucial discussions and comments. This work was partially supported by the NNSF key project of China under grant No. 10935013, the National Basic Science Program (Project 973) of China under grant No. 2010CB833004, CQ CSTC under grant No. 2009BA4050 and CQ CMEC under grant No. KJTD201016. ENS wishes to thank C.M.P. of Chongqing University of Posts and Telecommunications, for the hospitality during the preparation of the manuscript. GL would like to thank the MES of Cuba

for partial financial support of this investigation, and his research was also supported by the National Basic Science Program (PNCB) of Cuba and Territorial CITMA Project (No. 1115).

Appendix A: Stability of the finite critical points

For the critical points (x_c, y_c, z_c) of the autonomous system (24), the coefficients of the perturbation equations form a 3×3 matrix \mathbf{Q} , which reads:

$$\begin{aligned}
Q_{11} &= \frac{9x^2 - 3y^2}{2 + 2z^2 \operatorname{sgn}(\xi)} + \frac{4\sqrt{6}xz\sqrt{|\xi|} \operatorname{sgn}(\xi)}{2 + z^2 \operatorname{sgn}(\xi)} - \frac{3}{2} \\
Q_{12} &= y \left[\sqrt{6}\lambda - \frac{3x}{1 + z^2 \operatorname{sgn}(\xi)} \right] \\
Q_{13} &= -\frac{2\sqrt{6} [z^2 \operatorname{sgn}(\xi) - 2] \sqrt{|\xi|} x^2 \operatorname{sgn}(\xi)}{[2 + z^2 \operatorname{sgn}(\xi)]^2} + \frac{3(y^2 - x^2) z x \operatorname{sgn}(\xi)}{[1 + z^2 \operatorname{sgn}(\xi)]^2} - \sqrt{6}\sqrt{|\xi|} \operatorname{sgn}(\xi) \\
Q_{21} &= \frac{3xy}{1 + z^2 \operatorname{sgn}(\xi)} - \frac{\sqrt{\frac{3}{2}}y [\lambda z^2 \operatorname{sgn}(\xi) - 4z\sqrt{|\xi|} \operatorname{sgn}(\xi) + \lambda]}{1 + z^2 \operatorname{sgn}(\xi)} \\
Q_{22} &= \frac{3 + 3x^2 - \sqrt{6}\lambda x - 9y^2}{2 + 2z^2 \operatorname{sgn}(\xi)} + \frac{\left\{ 3z + \sqrt{6}x [4\sqrt{|\xi|} - \lambda z] \right\} z \operatorname{sgn}(\xi)}{2 + 2z^2 \operatorname{sgn}(\xi)} \\
Q_{23} &= \frac{y \operatorname{sgn}(\xi) \left\{ 3z(y^2 - x^2) + 2x\sqrt{6}\sqrt{|\xi|} [1 - z^2 \operatorname{sgn}(\xi)] \right\}}{[1 + z^2 \operatorname{sgn}(\xi)]^2} \\
Q_{31} &= \sqrt{6}\sqrt{|\xi|} \\
Q_{32} &= 0 \\
Q_{33} &= 0.
\end{aligned}$$

Despite the above complicated form, we can straightforwardly see that using the explicit critical points presented in Table I, the matrix \mathbf{Q} acquires a simple form that allows for an easy calculation of its eigenvalues. The corresponding eigenvalues ν_i ($i = 1, 2, 3$) for each critical point are presented in table III.

Thus, by determining the sign of the real parts of these eigenvalues, we can classify the corresponding critical point. In particular, if all the eigenvalues of a critical point have negative real parts then the corresponding point is stable, if they all have positive real parts then it is unstable, and if they change sign then it is a saddle point.

Appendix B: Stability of the critical points at infinity

Let us consider the Poincaré variables

$$x_r = \rho \cos \theta \sin \psi, \quad z_r = \rho \sin \theta \sin \psi, \quad y_r = \rho \cos \psi, \quad (\text{B1})$$

where $\rho = \frac{r}{\sqrt{1+r^2}}$, $r = \sqrt{x^2 + y^2 + z^2}$, $\theta \in [0, 2\pi]$, and $-\frac{\pi}{2} \leq \psi \leq \frac{\pi}{2}$ [21, 22]⁴. Thus, the points at “infinite” ($r \rightarrow +\infty$) are those having $\rho \rightarrow 1$. Furthermore, the physical phase-space is given by the intersection of the regions $2(x_r^2 + y_r^2) \leq 1$, $x_r^2 + y_r^2 - z_r^2 \geq 0$ and the circle

⁴ We restrict the angle ψ to this interval since the physical region is given by $y > 0$.

Cr. Point	Exists for	ν_1	ν_2	ν_3
A	all ξ, λ	$\frac{3}{2}$	$\frac{1}{4}(-3 - \sqrt{9 - 96\xi})$	$\frac{1}{4}(-3 + \sqrt{9 - 96\xi})$
B	$\xi = 0$, all λ	3	$3 - \sqrt{\frac{3}{2}\lambda}$	0
C	$\xi = 0$, all λ	3	$3 + \sqrt{\frac{3}{2}\lambda}$	0
D	$\xi = 0$, $\lambda^2 \leq 6$	$\lambda^2 - 3$	$\frac{1}{2}(\lambda^2 - 6)$	0
E	$\xi = 0$, $\lambda^2 \geq 3$	$\frac{3}{4}\left(-1 + \frac{\sqrt{24\lambda^2 - 7\lambda^4}}{\lambda^2}\right)$	$\frac{3}{4}\left(-1 - \frac{\sqrt{24\lambda^2 - 7\lambda^4}}{\lambda^2}\right)$	0
F	$\lambda^2 \leq \xi$	-3	$\frac{-3 + \sqrt{9 - 24\sqrt{\xi^2 - \lambda^2\xi}}}{2}$	$\frac{-3 - \sqrt{9 - 24\sqrt{\xi^2 - \lambda^2\xi}}}{2}$
G	$\lambda^2 \leq \xi$ or $\xi < 0$	-3	$\frac{-3 + \sqrt{9 + 24\sqrt{\xi^2 - \lambda^2\xi}}}{2}$	$\frac{-3 - \sqrt{9 + 24\sqrt{\xi^2 - \lambda^2\xi}}}{2}$
J	$\xi \neq 0$ and $\lambda = 0$	-3	$\frac{-3 + \sqrt{9 - 24\xi}}{2}$	$\frac{-3 - \sqrt{9 - 24\xi}}{2}$

TABLE III: The eigenvalues of the matrix \mathbf{Q} of the perturbation equations of the autonomous system (24). Points *B-E* exist only for $\xi = 0$, and for these points the variable z is zero and thus irrelevant. Although for these points the eigenvalue associated to the z -direction is zero, the stability conditions are obtained by analyzing the eigenvalues of the non-trivial 2×2 submatrix of \mathbf{Q} .

Cr. Point	Exists for	ν_1	ν_2
K_{\pm}	$\xi > 0$, all λ	$\frac{1}{2}\left(3 - \sqrt{96\xi - 24\sqrt{6\xi} + 9}\right)$	$\frac{1}{2}\left(3 + \sqrt{96\xi - 24\sqrt{6\xi} + 9}\right)$
L_{\pm}	$\xi > 0$, all λ	$\frac{1}{2}\left(3 - \sqrt{96\xi + 24\sqrt{6\xi} + 9}\right)$	$\frac{1}{2}\left(3 + \sqrt{96\xi + 24\sqrt{6\xi} + 9}\right)$

TABLE IV: The eigenvalues of the matrix \mathbf{Q} of the perturbation equations of the autonomous system (B2), calculated for the four critical points at infinity. Since we are restricted to the invariant set $y_r = 0$, \mathbf{Q} is a 2×2 matrix.

$x_r^2 + y_r^2 + z_r^2 \leq 1$, that is it is the region

$$\left\{ (x_r, y_r, z_r) \in [-1, 1] \times [0, 1] \times [-1, 1] \mid z_r^2 \leq x_r^2 + y_r^2 \leq \frac{1}{2} \right\}.$$

Performing the transformation (B1), in terms of the Poincaré variables the system (24) becomes:

$$\begin{aligned} x'_r &= \frac{2\sqrt{6\xi}(x_r^2 - 1)z_r x_r^2}{z_r^2 + 2(x_r^2 + y_r^2 - 1)} + \frac{3}{2}(2x_r^2 - 2y_r^2 - 1)x_r \\ &\quad + \frac{\sqrt{6\xi}[(2y_r^2 - 1)x_r^2 - y_r^2 + 1]z_r}{x_r^2 + y_r^2 - 1} \\ &\quad + \frac{\sqrt{\frac{3}{2}}\lambda y_r^2}{\sqrt{-x_r^2 - y_r^2 - z_r^2 + 1}}, \\ y'_r &= \frac{2\sqrt{6\xi}y_r z_r(-x_r^2 - y_r^2 - z_r^2 + 1)x_r^3}{(x_r^2 + y_r^2 - 1)[z_r^2 + 2(x_r^2 + y_r^2 - 1)]} \\ &\quad + \frac{1}{2}y_r(6x_r^2 + 4\sqrt{6\xi}z_r x_r - 6y_r^2 + 3) \\ &\quad - \frac{\sqrt{\frac{3}{2}}\lambda y_r x_r}{\sqrt{-x_r^2 - y_r^2 - z_r^2 + 1}}, \\ z'_r &= -\frac{4\sqrt{6\xi}(x_r^2 + y_r^2 - 1)x_r^3}{z_r^2 + 2(x_r^2 + y_r^2 - 1)} + \frac{2\sqrt{6\xi}y_r^2 z_r^2 x_r}{x_r^2 + y_r^2 - 1} \\ &\quad + \sqrt{6\xi}(2x_r^3 + x_r) + \frac{3(2x_r^4 - x_r^2 - 2y_r^4 + y_r^2)z_r}{2(x_r^2 + y_r^2 - 1)}. \end{aligned} \quad (\text{B2})$$

Transforming to spherical coordinates and taking the

limit $\rho \rightarrow 1$, the leading terms in (B2) are

$$\begin{aligned} \rho' &\rightarrow 0, \\ \sqrt{1 - \rho^2}\theta' &\rightarrow -\sqrt{\frac{3}{2}}\lambda \cos \psi \cot \psi \sin \theta, \\ \sqrt{1 - \rho^2}\psi' &\rightarrow \sqrt{\frac{3}{2}}\lambda \cos \theta \cos \psi. \end{aligned} \quad (\text{B3})$$

Since the equation for ρ decouples, it is adequate to investigate the subsystem of the angular variables. Therefore, the singular points at infinity satisfy

$$\begin{aligned} x_r &= \pm \cos \theta, \\ z_r &= \pm \sin \theta, \\ y_r &= 0, \end{aligned} \quad (\text{B4})$$

for some particular $\theta \in [0, 2\pi]$ that are determined as follows. Substituting (B4) in (B2) and solving for θ' we obtain

$$\theta' = -\frac{1}{2}\cos(2\theta)\left(3\cot\theta + 2\sqrt{6}\sqrt{\xi}\right). \quad (\text{B5})$$

This equation admits the parametric solution

$$\begin{aligned} \tau(\theta) &= c_1 + \frac{1}{9 - 24\xi} \left\{ 4\sqrt{6\xi} \tanh^{-1}(\tan \theta) \right. \\ &\quad \left. + 3\ln[\cos(2\theta)] - 6\ln[3\cos\theta + 2\sqrt{6\xi}\sin\theta] \right\}. \end{aligned}$$

Thus, the singular solutions with $\theta \in [0, 2\pi]$ are those satisfying $\theta = \frac{\pi}{4}, \frac{3\pi}{4}$, and $\cot \theta = -2\sqrt{\frac{2}{3}}\xi$, which due

to (B4) lead to simple expressions for x_r, y_r, z_r . These results are summarized in Table II.

In summary there are four physical critical points at infinity. The points K_{\pm} , satisfying $\theta = \frac{3\pi}{4}$ and the points L_{\pm} satisfying $\theta = \frac{\pi}{4}$. Thus, according to (B1), these critical points correspond to the limit $\phi \rightarrow \pm\infty, \dot{\phi}/H \rightarrow \pm\infty$ satisfying the rate

$$(\ln \phi)' \equiv \sqrt{6} \frac{x}{z} = \sqrt{6} \cot \theta.$$

Concerning the stability analysis of the singular points K_{\pm} and L_{\pm} , we take advantage that they are located in

the invariant set $y_r = 0$ and we examine their stability for the reduced 2D system x_r, z_r . The eigenvalues of the linearized 2D subsystem evaluated at K_{\pm} and L_{\pm} are displayed in Table IV, while the results of the stability analysis are presented in Table II.

Finally, we mention that mathematically there are two more critical points, namely the points P_{\pm} satisfying $\cot \theta = -2\sqrt{\frac{2}{3}}\xi$. However, they have no physical meaning since they give a divergent Ω_{DE} in (26), namely $\text{sign}[8\xi - 3] \cdot \infty$, and thus we do not consider them in the cosmological discussion.

-
- [1] A. G. Riess *et al.* [Supernova Search Team Collaboration], *Astron. J.* **116**, 1009 (1998); S. Perlmutter *et al.* [Supernova Cosmology Project Collaboration], *Astrophys. J.* **517**, 565 (1999); C. L. Bennett *et al.*, *Astrophys. J. Suppl.* **148**, 1 (2003).
- [2] S. 'i. Nojiri, S. D. Odintsov, [hep-th/0601213].
- [3] B. Ratra and P. J. E. Peebles, *Phys. Rev. D* **37**, 3406 (1988); C. Wetterich, *Nucl. Phys. B* **302**, 668 (1988); I. Zlatev, L. M. Wang and P. J. Steinhardt, *Phys. Rev. Lett.* **82**, 896 (1999); Z. K. Guo, N. Ohta and Y. Z. Zhang, *Mod. Phys. Lett. A* **22**, 883 (2007); S. Dutta, E. N. Saridakis and R. J. Scherrer, *Phys. Rev. D* **79**, 103005 (2009).
- [4] V. Sahni and S. Habib, *Phys. Rev. Lett.* **81**, 1766 (1998); J. P. Uzan, *Phys. Rev. D* **59**, 123510 (1999); V. Faraoni, *Phys. Rev. D* **62**, 023504 (2000); Y. G. Gong, *Class. Quant. Grav.* **19**, 4537-4542 (2002); E. Elizalde, S. Nojiri and S. Odintsov, *Phys. Rev. D* **70**, 043539 (2004); V. Faraoni, *Phys. Rev. D* **70**, 044037 (2004); M. R. Setare and E. N. Saridakis, *Phys. Lett. B* **671**, 331 (2009).
- [5] R. R. Caldwell, *Phys. Lett. B* **545**, 23 (2002); R. R. Caldwell, M. Kamionkowski and N. N. Weinberg, *Phys. Rev. Lett.* **91**, 071301 (2003); S. Nojiri and S. D. Odintsov, *Phys. Lett. B* **562**, 147 (2003); V. K. Onemli and R. P. Woodard, *Phys. Rev. D* **70**, 107301 (2004); E. N. Saridakis, *Nucl. Phys. B* **819**, 116 (2009); S. Dutta and R. J. Scherrer, *Phys. Lett. B* **676**, 12 (2009).
- [6] B. Feng, X. L. Wang and X. M. Zhang, *Phys. Lett. B* **607**, 35 (2005); Z. K. Guo, *et al.*, *Phys. Lett. B* **608**, 177 (2005); B. Feng, M. Li, Y.-S. Piao and X. Zhang, *Phys. Lett. B* **634**, 101 (2006); W. Zhao and Y. Zhang, *Phys. Rev. D* **73**, 123509 (2006); R. Lazkoz and G. Leon, *Phys. Lett. B* **638**, 303 (2006); R. Lazkoz, G. Leon and I. Quiros, *Phys. Lett. B* **649**, 103 (2007); E. N. Saridakis and J. M. Weller, *Phys. Rev. D* **81**, 123523 (2010); Y. -F. Cai, E. N. Saridakis, M. R. Setare, J. -Q. Xia, *Phys. Rept.* **493**, 1-60 (2010).
- [7] E. J. Copeland, M. Sami and S. Tsujikawa, *Int. J. Mod. Phys. D* **15**, 1753 (2006).
- [8] G. Leon, Y. Leyva, E. N. Saridakis, O. Martin and R. Cardenas, arXiv:0912.0542 [gr-qc], In *Dark Energy: Theories, Developments, and Implications*, Nova Science Publishers, (2010).
- [9] C. -Q. Geng, C. -C. Lee, E. N. Saridakis, Y. -P. Wu, *Phys. Lett. B* **704**, 384-387 (2011).
- [10] C. -Q. Geng, C. -C. Lee and E. N. Saridakis, *JCAP* **1201**, 002 (2012).
- [11] A. Einstein 1928, Sitz. Preuss. Akad. Wiss. p. 217; *ibid* p. 224; A. Unzicker and T. Case, arXiv:physics/0503046.
- [12] K. Hayashi and T. Shirafuji, *Phys. Rev. D* **19**, 3524 (1979); Addendum-*ibid.* **24**, 3312 (1982).
- [13] S. H. Chen, J. B. Dent, S. Dutta and E. N. Saridakis, *Phys. Rev. D* **83**, 023508 (2011). J. B. Dent, S. Dutta, E. N. Saridakis, *JCAP* **1101**, 009 (2011). Y. -F. Cai, S. -H. Chen, J. B. Dent, S. Dutta and E. N. Saridakis, *Class. Quant. Grav.* **28**, 2150011 (2011).
- [14] Weitzenböck R., *Invarianten Theorie*, (Nordhoff, Groningen, 1923).
- [15] J. W. Maluf, *J. Math. Phys.* **35** (1994) 335; H. I. Arcos and J. G. Pereira, *Int. J. Mod. Phys. D* **13**, 2193 (2004).
- [16] G. R. Bengochea and R. Ferraro, *Phys. Rev. D* **79**, 124019 (2009); E. V. Linder, *Phys. Rev. D* **81**, 127301 (2010); R. Myrzakulov, *Eur. Phys. J. C* **71**, 1752 (2011); P. Wu, H. W. Yu, *Eur. Phys. J. C* **71**, 1552 (2011); K. Bamba, C. -Q. Geng, C. -C. Lee, [arXiv:1008.4036 [astro-ph.CO]]; R. Zheng, Q. -G. Huang, *JCAP* **1103**, 002 (2011); K. Bamba, C. -Q. Geng, C. -C. Lee, L. -W. Luo, *JCAP* **1101**, 021 (2011); T. Wang, *Phys. Rev. D* **84**, 024042 (2011); K. K. Yerzhanov, S. R. Myrzakul, I. I. Kulnazarov and R. Myrzakulov, arXiv:1006.3879 [gr-qc]; R. -J. Yang, *Europhys. Lett.* **93**, 60001 (2011); P. Wu, H. W. Yu, *Phys. Lett. B* **693**, 415-420 (2010); G. R. Bengochea, *Phys. Lett. B* **695**, 405-411 (2011); P. Wu, H. W. Yu, *Phys. Lett. B* **692**, 176 (2010); B. Li, T. P. Sotiriou, J. D. Barrow, *Phys. Rev. D* **83**, 064035 (2011); Y. Zhang, H. Li, Y. Gong, Z. -H. Zhu, *JCAP* **1107**, 015 (2011); C. Deliduman and B. Yapiskan, arXiv:1103.2225 [gr-qc]; S. Chattopadhyay and U. Debnath, *Int. J. Mod. Phys. D* **20**, 1135 (2011); M. Sharif and S. Rani, *Mod. Phys. Lett. A* **26**, 1657 (2011) [arXiv:1105.6228 [gr-qc]]. M. Li, R. -X. Miao and Y. -G. Miao, *JHEP* **1107**, 108 (2011); H. Wei, X. -P. Ma and H. -Y. Qi, *Phys. Lett. B* **703**, 74 (2011); R. Ferraro and F. Fiorini, arXiv:1106.6349 [gr-qc]; R. -X. Miao, M. Li and Y. -G. Miao, *JCAP* **1111**, 033 (2011); C. G. Boehmer, A. Mussa and N. Tamanini, arXiv:1107.4455 [gr-qc]; H. Wei, H. -Y. Qi and X. -P. Ma, arXiv:1108.0859 [gr-qc]; S. Capozziello, V. F. Cardone, H. Farajollahi and A. Ravanpak, *Phys. Rev. D* **84**, 043527 (2011); P. Wu and H. Yu, *Phys. Lett. B* **703**, 223 (2011); M. H. Daouda, M. E. Rodrigues and M. J. S. Houndjo, arXiv:1109.0528 [physics.gen-ph]; K. Bamba and C. -

- Q. Geng, JCAP **1111**, 008 (2011); Y. -P. Wu and C. -Q. Geng, arXiv:1110.3099 [gr-qc]; P. A. Gonzalez, E. N. Saridakis, Y. Vasquez, [arXiv:1110.4024 [gr-qc]]; R. Ferraro and F. Fiorini, Phys. Rev. D **84**, 083518 (2011); C. G. Boehmer, T. Harko and F. S. N. Lobo, arXiv:1110.5756 [gr-qc], K. Karami and A. Abdolmaleki, arXiv:1111.7269 [gr-qc], H. Wei, X. -J. Guo and L. -F. Wang, Phys. Lett. B **707**, 298 (2012) [arXiv:1112.2270 [gr-qc]]; K. Atazadeh and F. Darabi, arXiv:1112.2824 [physics.gen-ph]; H. Farajollahi, A. Ravanpak and P. Wu, Astrophys. Space Sci. **338**, 23 (2012) [arXiv:1112.4700 [physics.gen-ph]]; M. Jamil, D. Momeni, N. S. Serikbayev and R. Myrzakulov, arXiv:1112.4472 [physics.gen-ph]; K. Karami and A. Abdolmaleki, arXiv:1201.2511 [gr-qc]; J. Yang, Y. -L. Li, Y. Zhong and Y. Li, arXiv:1202.0129 [hep-th]; M. H. Daouda, M. E. Rodrigues and M. J. S. Houndjo, arXiv:1202.1147 [gr-qc].
- [17] E. J. Copeland, A. R. Liddle and D. Wands, Phys. Rev. D **57**, 4686 (1998).
- [18] P.G. Ferreira, M. Joyce, Phys. Rev. Lett. **79**, 4740 (1997); Y. Gong, A. Wang and Y. -Z. Zhang, Phys. Lett. B **636**, 286 (2006); X. -m. Chen and Y. Gong, Phys. Lett. B **675**, 9 (2009); X. m. Chen, Y. g. Gong and E. N. Saridakis, JCAP **0904**, 001 (2009).
- [19] R. J. Scherrer and A. A. Sen, Phys. Rev. D **77**, 083515 (2008); R. J. Scherrer and A. A. Sen, Phys. Rev. D **78**, 067303 (2008); M. R. Setare and E. N. Saridakis, Phys. Rev. D **79**, 043005 (2009).
- [20] H. Wei, [arXiv:1109.6107 [gr-qc]].
- [21] S., Lynch, *Dynamical Systems with Applications using Mathematica*, Birkhauser, Boston (2007).
- [22] G. Leon, Class. Quant. Grav. **26**, 035008 (2009); G. Leon, P. Silveira and C. R. Fadrags, [arXiv:1009.0689 [gr-qc]], In *Classical and Quantum Gravity: Theory, Analysis and Applications*, Nova Science Publishers, (2010); G. Leon and C. R. Fadrags, *Cosmological Dynamical Systems*, LAP LAMBERT Academic Publishing, (2011).